IEEE Access
Multidisciplinary | Rapid Review | Open Access Journal

Received August 4, 2021, accepted August 10, 2021, date of publication August 24, 2021, date of current version August 31, 2021.

Digital Object Identifier 10.1109/ACCESS.2021.3107473

Cross-Modality Guided Contrast Enhancement for Improved Liver Tumor Image Segmentation

RABIA NASEEM[1], ZOHAIB AMJAD KHAN[2], (Student Member, IEEE), NITIN SATPUTE[3], AZEDDINE BEGHDADI[2], (Senior Member, IEEE), FAOUZI ALAYA CHEIKH[1], (Senior Member, IEEE), AND JOAQUÍN OLIVARES[4]

[1]Norwegian Colour and Visual Computing Laboratory, Norwegian University of Science and Technology, 7491 Gjøvik, Norway
[2]Laboratory of Information Processing and Transmission (L2TI), Institut Galilée, Université Sorbonne Paris Nord, 93430 Villetaneuse, France
[3]Department of Electrical and Computer Engineering, Aarhus University, 8000 Aarhus, Denmark
[4]Department of Electronic and Computer Engineering, Maimonides Biomedical Research Institute of Cordoba (IMIBIC), Universidad de Córdoba, 14071 Córdoba, Spain

Corresponding author: Rabia Naseem (rabia.naseem@ntnu.no)

This work was supported by the Project High Performance soft tissue Navigation (HiPerNav) through the European Union Horizon 2020 Research and Innovation Program under Grant 722068.

ABSTRACT Tumor segmentation in Computed Tomography (CT) images is a crucial step in image-guided surgery. However, low-contrast CT images impede the performance of subsequent segmentation tasks. Contrast enhancement is then used as a preprocessing step to highlight the relevant structures, thus facilitating not only medical diagnosis but also image segmentation with higher accuracy. In this paper, we propose a goal-oriented contrast enhancement method to improve tumor segmentation performance. The proposed method is based on two concepts, namely guided image enhancement and image quality control through an optimization scheme. The proposed OPTimized Guided Contrast Enhancement (OPTGCE) scheme exploits both contextual information from the guidance image and structural information from the input image in a two-step process. The first step consists of applying a two-dimensional histogram specification exploiting contextual information in the corresponding guidance image, i.e. Magnetic Resonance Image (MRI). In the second step, an optimization scheme using a structural similarity measure to preserve the structural information of the original image is performed. To the best of our knowledge, this kind of contrast enhancement optimization scheme using cross-modal guidance is proposed for the first time in the medical imaging context. The experimental results obtained on real data demonstrate the effectiveness of the method in terms of enhancement and segmentation quality in comparison to some state-of-the-art methods based on the histogram.

INDEX TERMS Guided enhancement, cross-modality, contrast enhancement, 2D histogram specification (HS), SSIM gradient, tumor segmentation.

I. INTRODUCTION

Liver cancer is the fifth most prevalent cancer in the world, carrying a low survival rate [1]. Nevertheless, timely detection of cancerous tumors and effective treatment strategies can improve the overall survival rate. Diagnostic imaging techniques such as CT facilitate timely diagnosis of cancer; however, low contrast and noise limit their utility [2]. Moreover, such low-contrast images make segmentation and tumor detection challenging problems that can be overcome by applying a contrast enhancement beforehand.

It is also worth mentioning here that a single medical imaging modality is unable to capture all the relevant structural information from the organs. For this reason, it is now becoming more common to acquire both CT and MR images periodically during liver cancer diagnosis and treatment [3]. Therefore, it would be interesting to use the additional captured information from one imaging modality (e.g. MRI) to enhance the other (e.g. CT). The concept of enhancing the image from one modality using cross-modal image

The associate editor coordinating the review of this manuscript and approving it for publication was Humaira Nisar.

information is not novel; similar ideas have been successfully applied to natural images [4]–[6]. One such approach for liver CT image enhancement using the corresponding MR images was proposed to improve the visibility of tumors and vessels [7]. In general, the cross-modality guided enhancement methods have shown better performance in comparison with the classic single image enhancement methods [8], [9].

Currently, there are two main challenges related to image enhancement in the medical context. Firstly, most recent enhancement techniques are tailored to only specific types of images. Secondly, it is not easy to find a well-established benchmark for evaluating the existing enhancement methods. For these reasons, the effectiveness of the enhancement approaches is often assessed based on their impact on the underlying application. For medical imaging, the motivation of CE, in general, is to improve the visual appearance of relevant organ structures for better diagnosis and intervention [10]. However, limited research has been done on image quality enhancement to improve the segmentation of such organ structures [4], [11]–[14]. By using CE as preprocessing step, improved segmentation of relevant structures in CT images could be achieved as concluded in [13]. Therefore, there is a dire need for efficient CE algorithms for such images.

Traditional enhancement methods suffer from limitations such as saturation, over-enhancement, and uneven contrast spatial distribution, that may result from the uncontrolled CE process. One way to overcome such limitations is to combine the contrast enhancement approach with a quality control scheme. Inspired by the guided filtering approach and the simplicity of context-aware histogram-based image quality enhancement, we propose in this paper a cross-modality guided histogram specification technique to improve the contrast of liver CT images using MRI images as guiding input data. Furthermore, optimization is incorporated to prevent the saturation artifacts inherent to histogram-based methods. A similar idea was proposed for enhancing natural images in [15]. It consists of mapping the histogram of the input image to that of a reference image combined with an optimization technique to preserve the structures of the input image. In this work, we propose a similar approach for medical images using cross-modal information. The new CE approach is hence based on two concepts, namely, cross-modality-guided medical image enhancement to improve the global contrast, and quality control to preserve the local structures during enhancement. Here, we formulate the cross-modal CE as an optimization problem, where the gradient of structural similarity index measure (SSIM) is used for local structure preservation and minimizing artifacts introduced during enhancement [16]. Later, the role of CE is analyzed in facilitating tumor segmentation. The overall processing scheme is evaluated on a real dataset containing CT and MRI of the human liver with segmentation ground truth. The main contributions of this paper are:

- The two-dimensional histogram specification-based CE process is formulated as an optimization problem and extended to multi-modal medical imaging data for the first time.
- SSIM gradient is incorporated in the optimized cross-modality guided 2D-HS framework to preserve structural fidelity of the enhanced image with the original image while applying enhancement.
- In order to obtain the objective of contrast enhancement without affecting the important structures of the image, the algorithm achieves a nice balance between retaining structural similarity with input image (by integrating SSIM gradient) and enhancing contrast by employing 2D entropy. The suggested combination of cross-modal guidance and quality control enhances the CT image exploiting contextual information, as opposed to context-unaware schemes.
- A new goal-oriented performance evaluation of the proposed approach is done utilizing objective quality metrics and through segmentation results applied on real multi-modal liver data. Comparison with single enhancement techniques validate the superior performance of the proposed method.

The rest of the paper is organized as follows. Section II provides a brief review of relevant contrast enhancement methods. Section III describes the proposed Optimized guided CE method. Experimental results of CE are discussed in section IV. The results of applying segmentation on the enhanced images are described in section V, followed by conclusion in section VI.

II. RELATED WORK

Among the methods for image quality enhancement, CE is the most intuitive and widely used solution in various fields of application, especially in medical imaging. Contrast enhancement methods can be broadly classified into two main categories: direct methods and indirect methods [17]. In the first category, the contrast is first defined and amplified to then deduce the modified value associated with the pixel to be treated. In the second category, the pixel value is transformed by means of an operation defined from global characteristics, such as the distribution of pixel values, or local characteristics such as the intensity gradient of the pixel. These operations can be performed in the spatial or transform domain or even in the joint spatial/spatial-frequency domain. It is well known that methods that operate in the transform domain and more particularly those that exploit multi-scale aspects and directional selectivity are more efficient but at the cost of increased complexity and prohibitive computation time in the case of large volumes of image data. It is therefore natural to turn to global methods and more specifically those that exploit the distribution of pixel values in the case of medical images. Among these methods, those based on histograms developed in general for natural images constitute an interesting alternative to other complex and time-consuming methods. Indeed, histogram-based CE approaches are well investigated both for natural as well as medical images, thanks to their low complexity and acceptable performance [18], [19]. For instance,

histogram equalization (HE) is one of the conventional histogram-based CE methods that map the global Cumulative Distribution Function (CDF) of the input image to that of a uniform distribution. Other histogram-based methods like Adaptive Histogram Equalization (AHE) and Contrast Limited Adaptive Histogram Equalization (CLAHE) operate on a small region around each pixel of the image to improve local contrast [20]. Besides these, another histogram-based approach, Histogram Specification (HS), uses CDF of the reference image with better perceptual quality to improve the visual appearance of a low contrast image [21], [22]. Similarly, another interesting histogram-based approach proposed for natural images uses contextual information through the 2D-CDF of the target image to exploit the inter-pixel correlation [23], [24]. This approach [23] has been shown to outperform other histogram-based approaches including minimum within-class variance multi-histogram equalization [25].

Among these histogram-based methods, some have also been used for medical image enhancement such as AHE and CLAHE for CE of FLuid Attenuated Inversion Recovery (FLAIR) MR images of brain [18]. In this method, the authors first performed contrast stretching before applying AHE/CLAHE. Eventually, to highlight abnormal hyperintense regions they have detected regional maxima followed by performing a local averaging of pixel values. However, their method is strictly application-specific and they have only used PSNR and average gradient for comparison, both of which are not suitable for performance evaluation of CE methods. Similarly, another histogram-based method to enhance CT images has combined normalized gamma correction with CLAHE to reduce the excessive brightness introduced by CLAHE [19]. In this work as well, the similarity metrics like SSIM [16] are inefficient for performance evaluation of CE methods, since there is no reference image in the CE task that can be used for similarity comparison. Few enhancement techniques [2], [26], [27] decompose the low-contrast image into detail and base layer separating high frequency and low-frequency contents in the image and apply histogram modification to enhance the base layer. The histogram is modified to prevent over-enhancement of the image by ensuring that the minimum gray level of the enhanced image approximates zero.

Despite the promising results of histogram-based methods in many applications, they sometimes introduce artifacts in the resulting image. Optimization strategies could be then used to reduce these side effects [28]. For instance, a HE-variant approach [29] finds an optimal threshold gray level value that separates the histogram into four sub-histogram. Histogram clipping is then applied to adjust the threshold according to the distribution of the original histogram. The proposed approach preserves naturalness of the image while minimizing over-enhancement. MedGA [30], another optimization-based technique was proposed to enhance the MR images. It is a combination of histogram-based method and genetic algorithm; however, only specific Region of Interest was enhanced in this way. Similarly, Lin *et al.* [31] achieved a nice balance between image brightness and contrast using a histogram averaging and remapping scheme. CE is conditioned by minimizing the average brightness difference between the input and enhanced images while maximizing the entropy in the processed image. However, this method is not well suited to dark images because of its inherent and fundamental brightness preserving property. Another method that maximizes information content and minimizes the artifacts has been proposed in [32]. The intermediate histogram equalized image and the original image are combined using a weighting factor computed by using a golden section search algorithm to attain uniform distribution. However, the local details are lost in case the image contains unevenly illuminated regions.

A breakthrough in the field of image enhancement was achieved when He *et al.* [33] introduced the idea to exploit information in a similar image to enhance the underlying image. This concept was further extended to cross-modality guided natural image enhancement [9]. The majority of cross-modality guided natural image enhancement methods process input images emanating from both modalities with the same contents and an accurate pixel to pixel correspondence, which largely simplifies the enhancement process [8]. Based on this strategy, Near Infrared (NIR) images were enhanced using photographs [34]. This method used gradient-based histogram matching to embed contrast of NIR images in photos. Moreover, wavelet domain processing was done to improve texture information. A similar idea was applied to medical images recently, where 2D HS was applied to map histogram of liver CT image to that of corresponding MR image [7]. However, optimization to control CE was not done in this work.

III. METHODOLOGY: OPTimized GUIDED CONTRAST ENHANCEMENT (OPTGCE)

Generally, classical Contrast Enhancement (CE) methods do not optimize an objective function or contrast-related measure; instead, they manipulate the pixel values according to a predefined distribution. Besides, these approaches amplify the contrast without objectively controlling the possible artifacts that may arise from the CE process. To the best of our knowledge, there are very few works where the contrast enhancement effect is controlled according to a well-defined framework. The proposed method OPTGCE operates according to this strategy. It applies HS-based CE to the low-contrast CT image based on the second-order distribution of an image of a complementary modality, that is MRI. The motivations behind the use of histogram-based methods are essentially their simplicity, reduced computational load, and the fact of exploiting a global statistical quantity that contains essential information on the distribution of pixel values. This is especially advantageous in the case of a large size of medical imaging data. Therefore, the 2D histogram effectively exploits the inter-pixel interactions, i.e. second-order statistics, in the design of the CE scheme.

This treatment enhances the overall contrast well but may suffer from some side effects. Indeed, the locally relevant structures of the image can be negatively affected, leading the processed image to be divergent from the original. Therefore, it is necessary to control the critical parameters of the CE process to amplify local contrast while simultaneously preserving the intrinsic structures of the image. One strategy to prevent the CE from side effects is to control the enhancement by using a local similarity measure between the input and enhanced image or some stopping criteria. Here, we perform the optimization using a measure that is directly related to the structural information in the image and carries contrast information. Furthermore, the extent of contrast is quantified through the two-dimensional entropy. The flowchart of the proposed technique is shown in Fig. 1. The three essential components of the proposed method, namely the 2D histogram specification-based CE, the structural gradient-based similarity measure, and 2D entropy are described below.

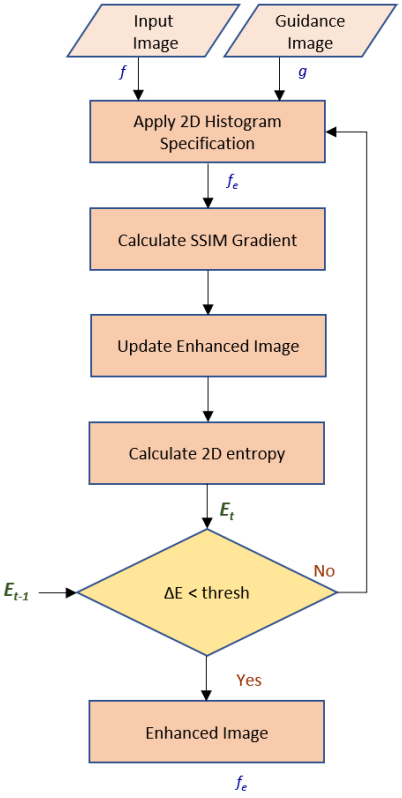

FIGURE 1. Flowchart of the proposed method.

A. 2D HISTOGRAM SPECIFICATION

Most image processing methods based on the distribution of pixel values involve only one-dimensional histogram. This has the disadvantage of not taking into account the strong spatial correlation of pixels and exploiting it in order to avoid side effects associated with histogram approaches. These limitations have led to the use of higher-order statistics of pixel values and characteristics to develop more efficient methods. The two-dimensional grayscale histogram is the simplest higher-order distribution. A two-dimensional histogram was then introduced in order to exploit the pixel inter-correlation in various image processing tasks such as image classification and grey-level thresholding [35], [36]. Later, this idea was also applied to 2D-HS and 2D-HE [23]. Indeed, it has been shown that the 2D HS clearly outperforms its one-dimensional HE and HS counterparts in terms of visual quality [23]. The approach in [23] is driven by the principle that the local and global contrast of the image could be enhanced by amplifying the grey-level transitions of neighboring pixels. One way to accentuate such transitions is to exploit the grey-level transition probability, i.e. 2D grey-level histogram. In recent work, 2D-HS based approach was applied to improve the contrast of liver CT images using MR images [7]. Although this method produces an acceptable enhancement, it is accompanied by a darkening or brightening effect in certain areas of the image due to the use of top hat and bottom hat transforms [37].

For the sake of completeness of the article, we recall here the basic notions and concepts introduced in the methods of 2D histogram specification. Let us consider an input image $[f] = \{f(m,n)|1 \leq m \leq M, 1 \leq n \leq N\}$, where $f(m,n)$ is the grey-level of pixel located at (m,n); the dynamic range of image is $[f_{min}, f_{max}]$ and $M \times N$ is its height and width respectively. The principle of guided contrast enhancement is to transform an input image $[f]$ into an output image $[f_e]$ to improve its contrast. The guide or reference image used in this process is represented by $[g]$, that is an image of better perceptual quality. One way to achieve this objective is to use the traditional Histogram Modification Framework and map the 1D-CDF of $[f]$ to that of $[g]$. However, as pointed out before, it is more efficient to consider pixel context, use higher-order statistics and compute the 2D-CDF instead when using the HS approach. Therefore, two-dimensional histograms of both guidance and input images, h_g and h_f respectively are derived from the Grey Level Co-occurrence Matrix (GLCM) computed from the two images. GLCM is a square matrix containing the number of occurrences of pairwise combinations of grey levels when exploring the whole image using a sliding window and a defined neighborhood. For the sake of simplicity, the neighborhood is generally restricted to the two nearest neighbors of the current pixel, i.e. left and above pixels. Let $f(m,n)$ denote the input image pixel's grey level. The GLCM is then computed as follows:

$$C_f(i,j) = \sum_{i=0}^{K-1} \sum_{j=0}^{K-1} \delta_{ij}(f(m,n), f(p,q)), \tag{1}$$

Here, i and j represent the pixel values and (m,n) and (p,q) represent the image coordinates, K is the total number of grey levels, and $0 \leq i,j \leq K-1$,

$$\delta_{ij}(a,b) = \begin{cases} 1, & \text{if } i = a \text{ and } j = b \\ 0, & \text{otherwise} \end{cases}$$

The transition probability of grey-levels, i.e. the 2D normalized histogram, is derived from the GLCM as follows:

$$h_f(i,j) = \frac{C_f(i,j)}{\sum_{i=0}^{K-1}\sum_{j=0}^{K-1} C_f(i,j)} \tag{2}$$

The 2D-histogram is then used in the pixel grey-level mapping process using the histogram specification method as described below. This mapping process is based on the two-dimensional Cumulative Distribution Function (CDF) of the input and guidance images computed as follows.

$$H_f(i,j) = \sum_{i=0}^{K-1}\sum_{j=0}^{K-1} h_f(i,j) \tag{3}$$

The expression of the 2D-CDF of the guidance image is computed similarly and is represented as H_g. Once the 2D-CDF of both images is computed, the transformation T allowing the mapping between the input signal and the desired signal is obtained as follows:

$$T(i,j) = \arg\min_{[k,l]} |H_f(i,j) - H_g(k,l)| + \eta(|i-k| + |j-l|) \tag{4}$$

The mapping is accomplished by searching the target pixel values, $T(i,j)_1$ and $T(i,j)_2$ corresponding to pixel values i and j in $[f]$. The second term in Eq. 4, i.e. $|i-k| + |j-l|$ ensures to select a nearby pixel pair for which the difference between both CDFs among the candidate pixel values is minimized. η represents a very small number and its value $= 10^{-4}$.

The final step in 2D-HS consists of mapping the intensity values in $[f]$ to new values. To this end, each pixel and its immediate neighbor are considered. The intensity values for the enhanced image $[f_e]$ are therefore calculated using the equation below:

$$f_e(m,n) = T(f(m,n), f(m,n+1)) \tag{5}$$

From Eq. 5, it can be inferred that transformation of each value in the original image $[f]$ to a new value in the enhanced image $[f_e]$ also depends on its neighboring element. Therefore, unlike the 1D histogram specification which only considers individual pixel values for calculating the CDFs and ultimately mapping these values, this approach also exploits the contextual information among the pixels. Next, we look at the SSIM gradient approach.

B. GRADIENT BASED STRUCTURAL SIMILARITY MEASURE

As mentioned above, histogram specification is widely applied to enhance image contrast. However, like many transformation-based CE methods relying on global statistical descriptors, it affects local and global image structures. One way to control processing distortions is to integrate into the CE process a stopping criteria or an objective function and formulate the whole problem in a constrained optimization framework. The method proposed by Avanaki [15] belongs to this kind of solution. The idea is to apply global HS to a low-contrast image driven by an SSIM-based measure to control the enhancement through structural similarity changes between the original image and its enhanced variant. SSIM is a well-established measure to calculate the extent of similarity between two images [16]. Considering one image as a reference, the index provides the quality of the image under analysis in comparison with a reference. SSIM index is calculated between corresponding local blocks in images $[A]$ and $[B]$, after which the average of the values is taken to obtain a single value of SSIM as the overall similarity index. Let us assume that a_x and b_x represent corresponding blocks x in both images; μ_{a_x} and μ_{b_x} represent the mean intensity values of a_x and b_x and the standard deviations are given by σ_{a_x} and σ_{b_x}. C_1 and C_2 are small numbers greater than 0 to ensure the denominator is not zero. The SSIM between the two blocks a_x and b_x is then expressed as:

$$\mathrm{SSIM}(a_x,b_x) = \frac{\left(2\mu_{a_x}\mu_{b_x}+C_1\right)\left(2\sigma_{a_xb_x}+C_2\right)}{\left(\mu_{a_x}^2+\mu_{b_x}^2+C_1\right)\left(\sigma_{a_x}^2+\sigma_{b_x}^2+C_2\right)} \tag{6}$$

Few terms in Eq. 6 are described mathematically as:

$$\begin{aligned} \mu_{a_x} &= w * a_x, \\ \sigma_{a_xb_x} &= w * (a_x b_x) - \mu_{a_x}\mu_{b_x}, \\ \sigma_{a_x}^2 &= w * a_x^2 - \mu_{a_x}^2 \end{aligned} \tag{7}$$

where w is 11×11 Gaussian kernel and $*$ indicates convolution. Eq. 6 could be regarded as expression for SSIM index map, $\mathrm{SSIM}_{\mathrm{map}}$ calculated via element wise addition and multiplication using parameters expressed in Eq. 7. Then, at all points, $\mathrm{SSIM}_{\mathrm{map}}$ indicates local similarity between images $[A]$ and $[B]$. The global SSIM index for the overall images can then be expressed as:

$$\mathrm{SSIM}(A,B) = \frac{1}{Z}\sum_{\forall x} \mathrm{SSIM}_{\mathrm{map}}(a_x, b_x; x) \tag{8}$$

where Z denotes the number of pixels in either image. $\mathrm{SSIM}_{\mathrm{map}}(a_x, b_x; x)$ is SSIM index value corresponding to the window x of size c $\times$ c in images $[A]$ and $[B]$, starting from the upper left corner of images and proceeding to the bottom right. For the local SSIM measures in Eq. 6, we define the following terms for compactness:

$$\begin{aligned} \alpha_1(a_x,b_x) &= 2\mu_{a_x}\mu_{b_x} + C_1, \\ \alpha_2(a_x,b_x) &= 2\sigma_{a_xb_x} + C_2 \end{aligned} \tag{9a}$$

$$\begin{aligned} \beta_1(a_x,b_x) &= \mu_{a_x}^2 + \mu_{b_x}^2 + C_1, \\ \beta_2(a_x,b_x) &= \sigma_{a_x}^2 + \sigma_{b_x}^2 + C_2 \end{aligned} \tag{9b}$$

As discussed earlier, the SSIM gradient-based optimization method [15] is applied to the cross-modal medical image enhancement in this work. Here, 2D-HS is applied to enhance CT images by exploiting the better quality of MR images. When applied in the framework of optimization, the SSIM gradient refines the enhancement process incrementally.

The integration of SSIM ultimately preserves the overall morphology of the original image with minimal information

TABLE 1. Description of important notations used in the paper.

Symbol	Description
$f(m,n)$	Gray level in the input image $[f]$ at location (m,n)
$g(m,n)$	Gray level in the guidance image $[g]$ at location (m,n)
f_e	Enhanced output image
K	Total number of gray levels in images $[f]$ or $[g]$
M,N	Total number of rows and columns respectively in either image $[f]$ or $[g]$
$C_f(i,j)$	Co-occurrence matrix corresponding to image $[f]$
h_f	Probability Density Function (2D) associated with $[f]$
H_f	Cumulative Distribution Function (2D) associated with $[f]$
$T(i,j)$	Transformation Matrix
a_x, b_x	Neighborhood /Blocks of images $[A]$ and B respectively (size $c \times c$) defined for SSIM calculation
x	Window/ Block number in the images $[A]$ and $[B]$ for SSIM
$\text{SSIM}(A,B)$	SSIM value between images $[A]$ and $[B]$
$\partial_{\mathbf{f_e}} \text{SSIM}(f,f_e)$	SSIM gradient of image $[f_e]$ with respect to image $[f]$
Z	Total number of pixels in either image $[f]$ or $[g]$ (both are same size)
μ_a	Mean intensity value of window a in image $[A]$
σ_a^2	Variance of block a in image $[A]$
E_t	Two-dimensional entropy of enhanced image $[f_e]$ at iteration t
t	Total number of times the proposed algorithm runs
ΔE	Change in entropy between successive iterations
$\Delta SSIM(t)$	Increase in SSIM value at iteration t
α	Step size used to update image using SSIM gradient

loss during enhancement. Here, we denote the input image as $[f]$ and the image whose structural similarity is being compared with $[f]$ as $[f_e]$; $[f_e]$ is obtained after applying 2D-HS. Now, to adapt the notion of SSIM gradient to our scenario, let us replace $[A]$ by $[f_e]$ and $[B]$ by $[f]$ and rewrite Eq. 8 as:

$$\text{SSIM}(f_e,f) = \frac{1}{Z}\sum_{\forall x} \text{SSIM}_{\text{map}}(f_{e_x}, f_x; x) \tag{10}$$

Calculating the derivative of Eq. 10 with reference to $[f_e]$ gives the SSIM gradient expression as follows:

$$\begin{aligned}\partial_{f_e}\,&\text{SSIM}(f_e,f)\\ &= \frac{2}{Z}\left[\left(w * \frac{\alpha_1}{\beta_1\beta_2}\right) f\right]\\ &\quad + \left(w * \frac{-\text{SSIM}_{\text{map}}}{\beta_2}\right) f_e\\ &\quad \times \left[+w * \frac{\mu_{f_e}(\alpha_2-\alpha_1) - \mu_f(\beta_2-\beta_1)\,\text{SSIM}_{\text{map}}}{\beta_1\beta_2}\right]\end{aligned} \tag{11}$$

where α_1, α_2, β_1 and β_2 have been described in Eq. 9a and 9b. Eq. 11 is a closed form solution and simple expression for SSIM gradient obtained by decomposing SSIM in linear terms. For thorough understanding of the mathematical computations, the reader is referred to [15]. The important notations used in this paper are listed in Table 1.

C. CONTRAST ENHANCEMENT WITH QUALITY CONTROL

After briefly introducing 2D-HS and SSIM gradient methods, the OPTGCE method is described in this subsection. Initially, we set the input CT image $[f]$ equal to $[f']$ and guidance MRI as $[g]$. The CDFs of $[f]$ and $[g]$ are calculated using Eq. 3. Eq. 4 mathematically defines how to calculate the transformation matrix T. The pixel values in $[f']$ are mapped to new values using Eq. 5 to get enhanced image $[f_e]$ in the manner explained in the section III-A. The proposed algorithm then calculates the structural similarity between $[f_e]$ and $[f]$ using Eq. 6 followed by SSIM gradient calculation with respect to image $[f_e]$, represented by ∂_{f_e}. Afterwards, $[f']$ is updated as mentioned in step 5 of the algorithm 1. Images $[f']$ and $[f_e]$ are updated in every iteration, while $[g]$ remains unchanged. Since SSIM computes the quality over the local neighborhood, it is capable of capturing local dissimilarities better than global approaches. Hence, optimizing the enhancement process using SSIM gradient offers better outcomes in terms of retaining the structure of the original image $[f]$. Algorithm 1 describes the steps of our proposed approach:

In the above algorithm, α represents the step size or the factor by which $[f_e]$ is updated in every iteration. Next, we describe a method to calculate the optimal value of α.

1) CALCULATION OF SUITABLE STEP SIZE

In this subsection, we elaborate the empirical approach similar to [15] for calculating an optimal step size α, so the algorithm attains higher SSIM in fewer iterations. The estimated increase in SSIM at iteration t is mathematically described as:

$$\Delta\,\text{SSIM}(t) = \alpha Z \sum_{\forall x} \left(\partial_{f_e}\,\text{SSIM}(f, f_e(t))\right)^2 \tag{12}$$

Based on the behavior of $SSIM(t)$ at several iterations, $\Delta\,\text{SSIM}(t)$ can be modeled by $\alpha r s^t$ [15]. The final value of SSIM (after several iterations) can be expressed as:

$$\text{SSIM}_{\text{f}} = \text{SSIM}' + \frac{r\alpha Z}{1-s} \tag{13}$$

Algorithm 1 OPTimized Guided Contrast Enhancement Algorithm (OPTGCE)

input CT image $= f$ and guidance image $= g$
Calculate 2D-CDF of guidance image as H_g and that of input image as H_f.
Set $f' = f$, $threshold = 0.05$ and $t = 1$
while $\Delta E >=$threshold **do**
1) Apply 2D histogram specification to f' to match 2D histogram of image g and generate enhanced image f_e.
2) Calculate structural similarity between f_e and f, SSIM(f, f_e) and SSIM gradient ∂_{f_e}SSIM(f, f_e)
3) Calculate E_t and ΔE.
4) Increment t as $t = t + 1$
5) Update f' contents using SSIM gradient driven factor as: $f' = f_e + \alpha Z \partial_{f_e}$SSIM$(f, f_e)$.

end while
Output enhanced image f_e

where $r = \sum_{\forall x} \left(\partial_{f_e} \text{SSIM}(f, f_e(1))\right)^2$, $s = \Delta\,\text{SSIM}(2)/\Delta\,\text{SSIM}(1)$, $\Delta\,\text{SSIM}(2)$ and $\Delta\,\text{SSIM}(1)$ denote the increase in SSIM values at $t = 2$ and $t = 1$ respectively. SSIM$'$ denotes the initial value of SSIM computed after first iteration. Our experiments show that SSIM value changes faster in earlier iterations, therefore the algorithm is executed three times to calculate the quantities in Eq. 13. Replacing SSIM_f value by 1 (the ideal value) and substituting the above values in Eq. 13, the approximated upper bound on α can be calculated as:

$$\alpha = \frac{1 - s}{rZ}\left(1 - \text{SSIM}'\right) \tag{14}$$

In our experiments, the value of α was calculated for the middle slice of each volume; the same value was used for all the slices in that volume, since SSIM values between original image and corresponding enhanced images among all the slices of specific volume were very close. The range of α found for our dataset was $[20, 60]$. Furthermore, it is important to mention that for any value of α in the specified range, the SSIM index value improves compared to that obtained in the first iteration, i.e. without incorporating SSIM gradient.

As stated in the previous sections, the objective of this work is to improve contrast while maintaining structural similarity with the input image to facilitate tumor segmentation. Therefore, along with ensuring this structural similarity (via SSIM gradient), we incorporate another criterion in our proposed method to measure the contrast enhanced at each iteration by applying 2D-HS. Therefore, 2D entropy is used to control the level of enhancement. The stopping criterion for the enhancement process is determined by the gain in two-dimensional entropy achieved for the enhanced image. The rationale of our methodology is to exploit inter-pixel correlation; therefore, we have used 2D entropy to formulate this criterion as:

$$E_t = -\sum_{i=0}^{K-1}\sum_{j=0}^{K-1} h_{f_{e_{(t)}}}(i,j)\ln(h_{f_{e_{(t)}}}(i,j)) \tag{15}$$

In Eq. 15, E_t represents the value of the 2D entropy for an image f_e at iteration t, where t varies from 1 to 10. $h_{f_{e_{(t)}}}(i,j)$ is the value of transition probability of gray level pairs. The change in entropy of the enhanced image gained with every iteration is calculated as follows:

$$\Delta E = E_t - E_{t-1} \tag{16}$$

Moreover, the change in entropy values (normalized to lie in the range [0,1]) across all the iterations is shown in Fig. 2 when the algorithm is applied to our dataset. Since the entropy values of all the images in a particular volume were very similar, entropy value of the middle slice from each volume is plotted for the sake of compactness. At a specific point in the optimization process, when ΔE becomes negligible (close to zero) or when the ΔE value starts oscillating, the enhancement process is stopped. Both these scenarios imply that further application of the enhancement process either will not further enhance the image or will likely introduce artifacts in the image. We observe an obvious increase in entropy when applying the proposed method for the first iteration. Subsequent applications bring a slow entropy increase; however, we show in section V that the segmentation accuracy is higher when segmentation is applied on images enhanced using the proposed algorithm. The result of applying the OPTGCE method and comparison with other methods is presented in the following section.

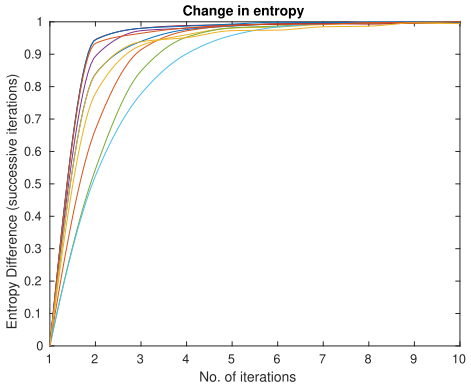

FIGURE 2. Variation in entropy values with iterations.

IV. ASSESSMENT OF CONTRAST ENHANCEMENT

In this section, we describe the dataset used in the experiment and the results obtained using different methods [7], [31], [32]. The qualitative and quantitative assessments are elaborated below.

A. DATASET

The data used in this research work is provided by the Intervention Center, Oslo University Hospital in Norway.

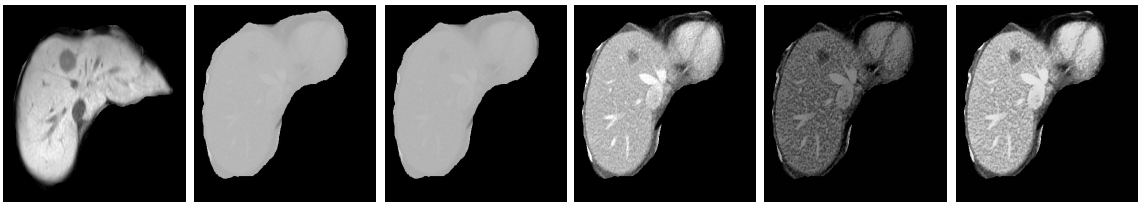

(a1) Guidance (a2) Input (a3) HEMIC (a4) AVHEQ (a5) CMGE (a6) OPTGCE

(a) Enhancement Results from state of the art methods

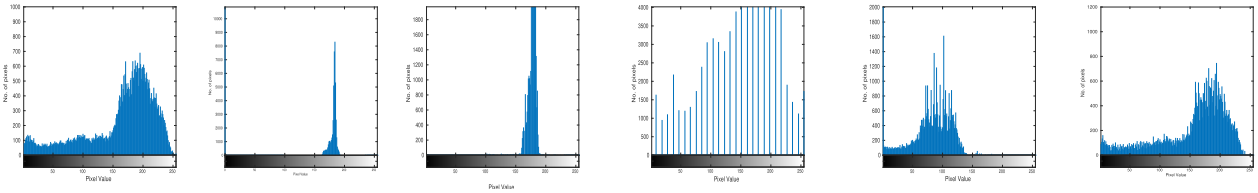

(b1) histogram a1 (b2) histogram a2 (b3) histogram a3 (b4) histogram a4 (b5) histogram a5 (b6) histogram a6

(b) Corresponding histograms of guidance, input and enhanced images

FIGURE 3. **Comparison of proposed method with state of the art methods and their corresponding histograms.**

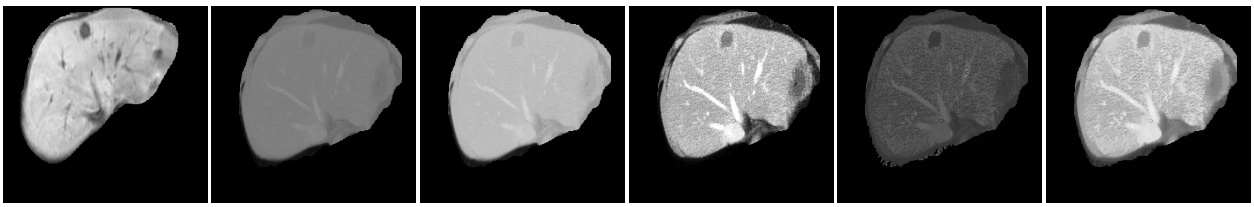

(a1) Guidance (a2) Input (a3) HEMIC (a4) AVHEQ (a5) CMGE (a6) OPTGCE

(a) Enhancement Results from state of the art methods

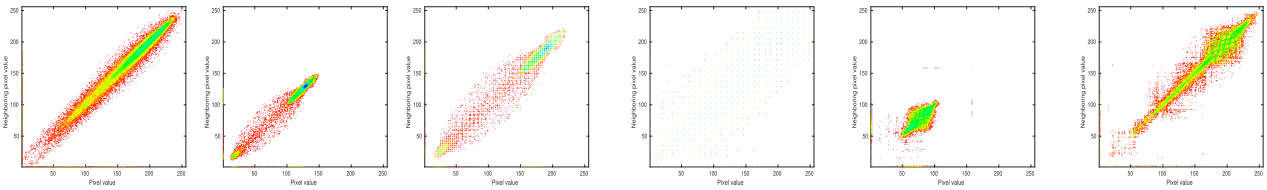

(b1) plot a1 (b2) plot a2 (b3) plot a3 (b4) plot a4 (b5) plot a5 (b6) plot a6

(b) Corresponding GLCM plots of guidance, input and enhanced images

FIGURE 4. **Comparison of proposed method with state of the art methods and their corresponding GLCM plots.**

Liver CT and MR data of the same patient are used; however, CT-MRI data is not registered since registration is not required for global enhancement methods. We tested our method on 10 patients' data constituting 99 CT-MR image pairs (containing tumors). The images from different volumes are of different spatial sizes (such as 512×512, 360×240) with pixel values in the range $[0, 255]$. In medical image processing tasks such as segmentation and enhancement, the processing is often restricted to a particular organ and the nearby organs are removed from the medical images [38], [39]. The liver area in the images is therefore separated and processing is applied only to this region.

1) QUALITATIVE ANALYSIS

In this subsection, few enhanced images alongwith their corresponding histograms and GLCM plots are presented in Fig. 3 and 4 respectively. To ensure a fair comparison, we selected all histogram based methods where [31] and [32] employ optimization based histogram processing and [7] applies cross-modality guided HS. We denote these methods as Averaging Histogram Equalization (AVHEQ) [31], Histogram Equalization with Maximum Intensity Coverage (HEMIC) [32] and Cross-Modality Guidance-based enhancement (CMGE) [7].

The input image in Fig. 3a2 has low contrast as validated by its histogram. Similarly, the input image in Fig. 4a2 is

TABLE 2. Quantitative assessment of different enhancement methods.

Dataset #	Entropy				MIGLCM			
	HEMIC [32]	AVHEQ [31]	CMGE [7]	OPTGCE	HEMIC [32]	AVHEQ [31]	CMGE [7]	OPTGCE
1	2.32	2.21	2.76	**3.13**	**1.1**	1.07	0.95	**1.1**
2	1.58	1.7	1.74	**2.4**	0.93	0.9	0.86	**1.12**
3	1.7	1.6	1.7	**1.9**	0.93	0.92	0.91	**1.06**
4	2.03	1.95	2.72	**3.00**	1.22	1.21	1.27	**1.4**
5	2.51	2.45	3.43	**3.62**	1.16	1.12	1.07	**1.31**
6	1.54	1.51	1.92	**2.12**	0.86	0.85	0.82	**0.98**
7	2.61	2.52	3.23	**3.64**	1.28	1.24	1.14	**1.42**
8	1.52	1.46	1.94	**2.1**	0.82	0.81	0.75	**0.94**
9	1.43	1.36	1.67	**1.88**	0.78	0.77	0.75	**0.81**
10	1.11	1.11	1.32	**1.41**	0.64	0.62	0.63	**0.76**

low-contrast CT image. The images enhanced using HEMIC (Fig. 3a3 and 4a3) do not show noticeable contrast improvement. Although CMGE (Fig. 3a5) expands the dynamic range of the image (Fig. 3a5), it darkens the image. AVHEQ (Fig. 4a4) stretches the dynamic range of enhanced images, however, its GLCM plot (Fig. 4b4) shows significant gaps among the pixel pairs and consequently the compactness of the plot is lost. The plot of OPTGCE enhanced image (Fig. 4b6) reflects the uniform distribution of the pixel pairs. Furthermore, it approximates the plot of the guidance image (Fig.4b1) in evenly distributing the pixel pairs; this similarity is also verified in their histograms (Fig. 3b1 and Fig. 3b6).

2) QUANTITATIVE ANALYSIS

Image Quality Assessment (IQA) is a well-investigated research field especially in the case of natural images [40]. However, the use of existing IQA metrics has serious limitations in the medical context [41]. The objectives of CE in the medical context are quite different [42], [43]. While in the case of natural images the objective is to measure the effect of various distortions on the perceptual quality of the image; in the medical context even if some degradation may disturb the radiologists the focus is rather on the diagnosis. Therefore, the existing IQA metrics must be used with special care. Another challenging topic is how to evaluate the performance of a given image quality enhancement algorithm in terms of perceptual quality [44]. In the present study, we focus on some contrast enhancement evaluation (CEE) metrics.

The motivation of the OPTGCE is to emphasize the appearance of specific structures in the image and convey the maximum structural information to facilitate tumor segmentation. To this end, we have chosen three different CEE metrics to evaluate the quality of enhanced images. The first metric is a mutual information-based no reference metric called MIGLCM [45]. This metric offers quantitative criteria that examines the changes in the statistical features, joint entropy, and mutual information, acquired from the GLCM of the original and the enhanced images. Besides MIGLCM, we have used a recent metric Multi-Criteria Contrast Enhancement Evaluation (MCCEE) found to be effective for the evaluation of CE in CT images that have been enhanced to improve tumor segmentation [46]. It is a comprehensive metric as it not only measures improvement in contrast but also considers other evaluation criteria like over-enhancement. For MCCEE, four features are evaluated for each image corresponding to four different criteria. These criteria include contrast enhancement, structure preservation, lightness order preservation, and brightness preservation. Two of the four features corresponding to the structure and lightness order preservation are evaluated from the subband images after wavelet decomposition. MCCEE is finally evaluated using a trained Support Vector Regressor (SVR) with subjective quality scores or DICE from the subsequent segmentation. MCCEE here is applied on data of three patients only since the rest of the data from seven patients is used for training.

TABLE 3. Median MCCEE values for different methods.

Data.#	HEMIC [32]	AVHEQ [31]	CMGE [7]	OPTGCE
1	0.25	0.32	0.31	**0.34**
2	0.23	0.22	0.22	**0.26**
3	0.21	0.26	0.36	**0.56**

For the last metric, we have used entropy, which is often used in QA of medical image enhancement [31]. Table 2 lists the median values of MIGLCM and entropy, whereas Table 3 shows the MCCEE values. It is pertinent to mention that the higher the MCCEE score, the better enhancement result is; the range of MCCEE is [0,1]. Similarly, a higher value of MIGLCM reflects better performance of CE algorithms. Besides, higher entropy values also correspond to superior CE performance; however, there is no specified range for this metric. From the tabular results, we can observe that OPTGCE demonstrates the best performance. For MCCEE and entropy, CMGE, HEMIC, and AVHEQ are ranked low overall by the two QA metrics. In the case of MIGLCM, HEMIC is ranked as the second-best and CMGE gives the

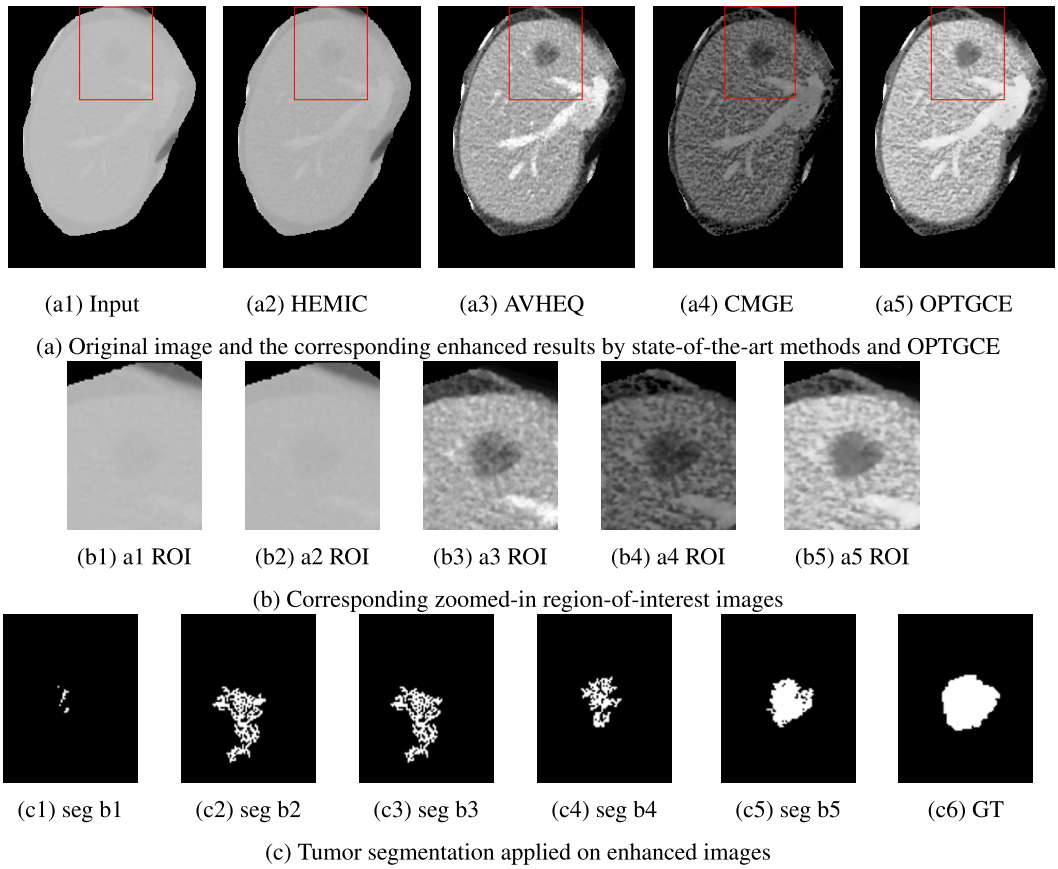

FIGURE 5. Comparison of tumor segmentation results with the ground truth.

poorest results. All in all, we observe that OPTGCE shows the best performance for all the quantitative metrics chosen. In this section, we compared the performance of our proposed method individually without looking at its effect on the subsequent segmentation task. In the following section, the application of the gradient-driven Seeded Region Growing (SRG) method on the enhanced images will be discussed.

V. TOWARDS AN OPTIMAL SEGMENTATION PRESERVING LOCAL STRUCTURES

Segmentation in low contrast medical images, particularly CT images is a delicate operation. The segmentation process is often accompanied by miss-classification errors that negatively impact high-level tasks, for instance, diagnosis in the medical context. Similar to several fields of scientific research, deep learning-based image segmentation approaches seem to dominate the state of the art [47]. However, DL-based techniques require an extensive amount of data to train the networks, which is difficult to acquire in the medical context due to confidentiality and ethical considerations. This work entails the segmentation of liver tumors from a rather limited volume of data consisting of only 99 liver tumor images (out of 10 patients' data). We, therefore, resort to the traditional approach, SRG. Several studies report the use of SRG for segmenting medical images compared to more sophisticated approaches [48]–[50]. However, as has been pointed out, classical segmentation, whether stochastic or deterministic, inevitably induces pixel classification errors, which could be fatal in the case under study here. One solution to minimize these errors is to apply pre-processing so as to amplify the inter-pixel gradient to facilitate the discrimination of local structures. Contrast enhancement is the most intuitive solution. In this work, one of the segmentation methods that seems to us the most adequate is the region growing technique based on the gradient of pixel values [51]. Indeed, the fact of first carrying out CE amplifies the gradient, which results in putting the gradient-based region growing method in the most favorable conditions. A constraint that may limit the utility of this approach is the execution time; therefore, we use its parallel implementation as proposed in [13]. In this section, we present the results of applying segmentation on enhanced images along with its quantitative assessment.

A. QUANTITATIVE ASSESSMENT OF SEGMENTATION

The results of applying gradient-driven SRG algorithm on enhanced as well as input images are demonstrated in Fig. 5 and 6. It can be noticed that the tumor in the

(a1) Input (a2) HEMIC (a3) AVHEQ (a4) CMGE (a5) OPTGCE

(a) Original image and the corresponding enhanced results by state-of-the-art methods and OPTGCE

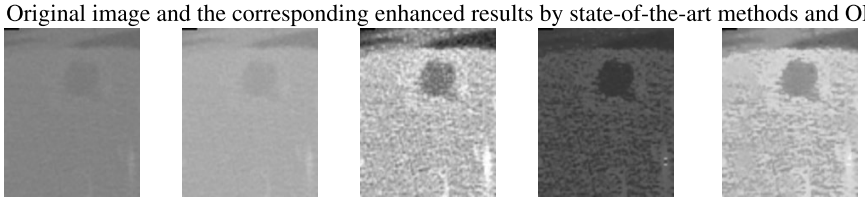

(b1) a1 ROI (b2) a2 ROI (b3) a3 ROI (b4) a4 ROI (b5) a5 ROI

(b) Corresponding zoomed-in region-of-interest images

(c1) seg b1 (c2) seg b2 (c3) seg b3 (c4) seg b4 (c5) seg b5 (c6) GT

(c) Tumor segmentation applied on enhanced images

FIGURE 6. **Comparison of tumor segmentation results with the ground truth.**

TABLE 4. **Comparison of different segmentation assessment method for enhancement results.**

Data	Input w/o processing			HEMIC [32]			AVHEQ [31]			CMGE [7]			OPTGCE		
	PPV	Dice	Haus.	PPV	Dice	Haus.	PPV	Dice	Haus.	PPV	Dice	Haus.	PPV	Dice	Haus.
vol1	**0.67**	0.16	14.21	0.63	0.26	23.5	0.66	0.173	17	0.56	0.36	14.6	**0.67**	**0.46**	**9.92**
vol2	**0.9**	0.14	8.66	0.83	0.26	8.26	0.86	0.27	7.7	0.88	0.38	7.3	**0.9**	**0.45**	**5.9**
vol3	0.85	0.31	16.18	0.85	0.36	15.78	0.86	0.42	14	0.83	0.48	12.47	**0.91**	**0.57**	**10.5**

input image can hardly be seen in Fig. 5a1 and 6a1 without applying CE. In general, application of the CE methods improve the contrast of the input image, which ultimately enables SRG to locate tumor contours favorably. However, OPTGCE well preserves uniformity in the structure of tumors in the enhanced image together with yielding sharp tumor edges. Therefore, Seeded Region Growing (SRG) algorithm is better able to locate the tumor contours in the OPTGCE-enhanced images. This property enables OPTGCE to outperform other CE methods in facilitating tumor segmentation. The quantitative segmentation assessment as well as qualitative comparison with ground truth also supports our claim.

It should be noted here that the segmentation results are demonstrated without applying any kind of post-processing such as morphological region filling. We believe that better results could be obtained if appropriate post-processing was applied to the segmented images. For further validation, we quantitatively evaluate the segmentation results using three assessment metrics, i.e., Positive Predictive Value (PPV), Dice and Hausdorff distance (with Euclidean distance). The average values of these metrics obtained for each volume are shown in Table 4. In the past, several metrics have been proposed to evaluate the performance of segmentation algorithms such as intensity-based, shape-based, and or distance-based. One of the challenges in medical image segmentation assessment is that the object of interest constitutes a small part of the image, therefore the assessment methods are biased to yield more weightage to specificity compared to sensitivity. Distance-based metrics such as Hausdorff distance are capable of detecting data outliers in such cases where intensity-based approaches may often fail. There is no standard range for the hausdorff distance values, however, the lower value indicates superior segmentation outcomes.

Among the numeric results in Table 4, PPV values in general are greater than 0.8 for all the segmentations. Since PPV computes the ratio between the number of pixels

correctly classified as tumors to the number of pixels correctly classified and the non-tumor pixels wrongly classified as tumors, this metric gives similar values to all the methods. It should be noted that the range of PPV metric is [0,1]; where 1 implies accurate segmentation. It can also be observed that all the segmentations in Fig. 5 and 6 do not include many non tumor pixels in the resultant segmentation when compared to the ground truth. Although Dice yields better scores for segmentation applied on images enhanced using the proposed method, the overall dice scores are low. Dice similarity metric gives higher value to the terms that compute the intersection between true positives in segmentation under test and ground truth. The range of dice score lies between 0 and 1, where 1 corresponds to the perfect segmentation. In the proposed CE approach, the segmented area does not completely overlap with the GT, contributing to lower dice scores; moreover, not applying any kind of post-processing to segmentation also introduces discontinuities and non uniformity in segmented tumors. It is worth mentioning here that the Dice scores are lowest when SRG algorithm is applied on the input images without any kind of enhancement, whereas Hausdorff distance shows highest value. The segmentation in the case of the OPTGCE method consistently achieves lower Hausdorff distance values for all three volumes. CMGE is the second-best while HEMIC ranks lowest in all the three cases tested.

VI. CONCLUSION

This study proposes an optimization-based guided contrast enhancement approach OPTGCE for low contrast CT images. The proposed technique adopts a context-aware 2D histogram-based scheme of exploiting information in the better perceptual quality guidance image for global contrast enhancement, while local image structures are enhanced through SSIM based measure in an optimization framework. This combination effectively improves the contrast while minimizing the artifacts associated with typical histogram-based enhancement methods to preserve the morphological information of the image during enhancement. The qualitative and quantitative analysis using metrics including entropy, MCCEE, and MIGLCM shows the superiority of the proposed method in comparison with the existing methods that do not include guidance mechanism. Finally, a tumor segmentation algorithm is applied on the enhanced images to analyze the performance of the proposed method in facilitating tumor segmentation. The comparison with the ground truth and quantitative assessment using Hausdorff distance, dice, and PPV metrics validate the superior performance of OPTGCE. With the availability of more data, goal-oriented contrast enhancement can be implemented using deep neural networks to facilitate tumor segmentation in different organs.

ACKNOWLEDGMENT

The authors thank the Intervention Centre, Oslo University Hospital, Norway, specially Ole Jakob Elle and Egidijuis Pelanis for providing images with ground truths to clinically validate tumor segmentation.

REFERENCES

[1] Y. Alvi, D. Regan, L. Schook, R. Gaba, and K. Schachtschneider, "Transcriptional regulation of alcohol induced liver fibrosis in a translational porcine hepatocellular carcinoma model," *Biochimie*, vol. 182, pp. 73–84, Mar. 2021.

[2] B. Sdiri, M. Kaaniche, F. A. Cheikh, A. Beghdadi, and O. J. Elle, "Efficient enhancement of stereo endoscopic images based on joint wavelet decomposition and binocular combination," *IEEE Trans. Med. Imag.*, vol. 38, no. 1, pp. 33–45, Jan. 2019.

[3] M. R. Oliva, "Liver cancer imaging: Role of CT, MRI, US and PET," *Cancer Imag.*, vol. 4, pp. S42–S46, Sep. 2004.

[4] B. Li and W. Xie, "Adaptive fractional differential approach and its application to medical image enhancement," *Comput. Electr. Eng.*, vol. 45, pp. 324–335, Jul. 2015.

[5] B. Kim, J. Ponce, and B. Ham, "Deformable kernel networks for joint image filtering," *Int. J. Comput. Vis.*, vol. 129, no. 2, pp. 579–600, Feb. 2021.

[6] Y. Li, J.-B. Huang, N. Ahuja, and M.-H. Yang, "Joint image filtering with deep convolutional networks," *IEEE Trans. Pattern Anal. Mach. Intell.*, vol. 41, no. 8, pp. 1909–1923, Aug. 2019.

[7] R. Naseem, F. A. Cheikh, A. Beghdadi, O. J. Elle, and F. Lindseth, "Cross modality guided liver image enhancement of CT using MRI," in *Proc. 8th Eur. Workshop Vis. Inf. Process. (EUVIP)*, Oct. 2019, pp. 46–51.

[8] X. Guo, Y. Li, J. Ma, and H. Ling, "Mutually guided image filtering," *IEEE Trans. Pattern Anal. Mach. Intell.*, vol. 42, no. 3, pp. 694–707, Mar. 2020.

[9] Q. Yan, X. Shen, L. Xu, S. Zhuo, X. Zhang, L. Shen, and J. Jia, "Cross-field joint image restoration via scale map," in *Proc. IEEE Int. Conf. Comput. Vis.*, Dec. 2013, pp. 1537–1544.

[10] Z. Al-Ameen and G. Sulong, "A new algorithm for improving the low contrast of computed tomography images using tuned brightness controlled single-scale Retinex," *Scanning*, vol. 37, no. 2, pp. 116–125, 2015.

[11] N. Satpute, R. Naseem, R. Palomar, O. Zachariadis, J. Gómez-Luna, F. A. Cheikh, and J. Olivares, "Fast parallel vessel segmentation," *Comput. Methods Programs Biomed.*, vol. 192, Aug. 2020, Art. no. 105430.

[12] W. Zhu, H. Jiang, E. Wang, Y. Hou, L. Xian, and J. Debnath, "X-ray image global enhancement algorithm in medical image classification," *Discrete Continuous Dyn. Syst.*, vol. 12, nos. 4–5, p. 1297, 2019.

[13] N. Satpute, R. Naseem, E. Pelanis, J. Gómez-Luna, F. A. Cheikh, O. J. Elle, and J. Olivares, "GPU acceleration of liver enhancement for tumor segmentation," *Comput. Methods Programs Biomed.*, vol. 184, Feb. 2020, Art. no. 105285.

[14] S. Survarachakan, E. Pelanis, Z. A. Khan, R. P. Kumar, B. Edwin, and F. Lindseth, "Effects of enhancement on deep learning based hepatic vessel segmentation," *Electronics*, vol. 10, no. 10, p. 1165, May 2021.

[15] A. N. Avanaki, "Exact global histogram specification optimized for structural similarity," *Opt. Rev.*, vol. 16, no. 6, pp. 613–621, Nov. 2009.

[16] Z. Wang, A. C. Bovik, H. R. Sheikh, and E. P. Simoncelli, "Image quality assessment: From error visibility to structural similarity," *IEEE Trans. Image Process.*, vol. 13, no. 4, pp. 600–612, Apr. 2004.

[17] A. Beghdadi and A. Le Negrate, "Contrast enhancement technique based on local detection of edges," *Comput. Vis. Graph. Image Process.*, vol. 46, no. 2, pp. 162–174, May 1989.

[18] I. S. Isa, S. N. Sulaiman, M. Mustapha, and N. K. A. Karim, "Automatic contrast enhancement of brain MR images using average intensity replacement based on adaptive histogram equalization (AIR-AHE)," *Biocybern. Biomed. Eng.*, vol. 37, no. 1, pp. 24–34, 2017.

[19] Z. Al-Ameen, G. Sulong, A. Rehman, A. Al-Dhelaan, T. Saba, and M. Al-Rodhaan, "An innovative technique for contrast enhancement of computed tomography images using normalized gamma-corrected contrast-limited adaptive histogram equalization," *EURASIP J. Adv. Signal Process.*, vol. 2015, no. 1, pp. 1–12, Dec. 2015.

[20] S. M. Pizer, E. P. Amburn, J. D. Austin, R. Cromartie, A. Geselowitz, T. Greer, and J. B. Zimmerman, "Adaptive histogram equalization and its variations," *Comput. Vis., Graph., Image Process.*, vol. 39, no. 3, pp. 355–368, 1987.

[21] C.-C. Sun, S.-J. Ruan, M.-C. Shie, and T.-W. Pai, "Dynamic contrast enhancement based on histogram specification," *IEEE Trans. Consum. Electron.*, vol. 51, no. 4, pp. 1300–1305, Nov. 2005.
[22] B. Xiao, H. Tang, Y. Jiang, W. Li, and G. Wang, "Brightness and contrast controllable image enhancement based on histogram specification," *Neurocomputing*, vol. 275, pp. 2798–2809, Jan. 2018.
[23] T. Celik, "Two-dimensional histogram equalization and contrast enhancement," *Pattern Recognit.*, vol. 45, no. 10, pp. 3810–3824, Oct. 2012.
[24] S. Jung, "Two-dimensional histogram specification using two-dimensional cumulative distribution function," *Electron. Lett.*, vol. 50, no. 12, pp. 872–874, 2014.
[25] D. Menotti, L. Najman, J. Facon, and A. D. A. Araujo, "Multi-histogram equalization methods for contrast enhancement and brightness preserving," *IEEE Trans. Consum. Electron.*, vol. 53, no. 3, pp. 1186–1194, Aug. 2007.
[26] Z. Huang, X. Li, N. Wang, L. Ma, and H. Hong, "Simultaneous denoising and enhancement for X-ray angiograms by employing spatial-frequency filter," *Optik*, vol. 208, Apr. 2020, Art. no. 164287.
[27] Z. Huang, Y. Zhang, Q. Li, T. Zhang, N. Sang, and H. Hong, "Progressive dual-domain filter for enhancing and denoising optical remote-sensing images," *IEEE Geosci. Remote Sens. Lett.*, vol. 15, no. 5, pp. 759–763, May 2018.
[28] Z. Huang, H. Fang, Q. Li, Z. Li, T. Zhang, N. Sang, and Y. Li, "Optical remote sensing image enhancement with weak structure preservation via spatially adaptive gamma correction," *Infr. Phys. Technol.*, vol. 94, pp. 38–47, Nov. 2018.
[29] Z. Huang, Z. Wang, J. Zhang, Q. Li, and Y. Shi, "Image enhancement with the preservation of brightness and structures by employing contrast limited dynamic quadri-histogram equalization," *Optik*, vol. 226, Jan. 2021, Art. no. 165877.
[30] L. Rundo, A. Tangherloni, M. S. Nobile, C. Militello, D. Besozzi, G. Mauri, and P. Cazzaniga, "MedGA: A novel evolutionary method for image enhancement in medical imaging systems," *Expert Syst. Appl.*, vol. 119, pp. 387–399, Apr. 2019.
[31] S. C.-F. Lin, C. Y. Wong, M. A. Rahman, G. Jiang, S. Liu, N. Kwok, H. Shi, Y.-H. Yu, and T. Wu, "Image enhancement using the averaging histogram equalization (AVHEQ) approach for contrast improvement and brightness preservation," *Comput. Elect. Eng.*, vol. 46, pp. 356–370, Aug. 2015.
[32] C. Y. Wong, S. Liu, S. C. Liu, M. B. Rahman, S. Lin, G. Jiang, N. Kwok, and H. Shi, "Image contrast enhancement using histogram equalization with maximum intensity coverage," *J. Mod. Opt.*, vol. 63, no. 16, pp. 1618–1629, 2016.
[33] K. He, J. Sun, and X. Tang, "Guided image filtering," in *Proc. ECCV*, 2010, pp. 1–14.
[34] S. Zhuo, X. Zhang, X. Miao, and T. Sim, "Enhancing low light images using near infrared flash images," in *Proc. IEEE Int. Conf. Image Process.*, Sep. 2010, pp. 2537–2540.
[35] R. M. Haralick, K. Shanmugam, and I. Dinstein, "Textural features for image classification," *IEEE Trans. Syst., Man, Cybern.*, vol. SMC-3, no. 6, pp. 610–621, Nov. 1973.
[36] F. Deravi and S. K. Pal, "Grey level thresholding using second-order statistics," *Pattern Recognit. Lett.*, vol. 1, nos. 5–6, pp. 417–422, Jul. 1983.
[37] J. C. Mello Roman, H. Legal-Ayala, and J. L. Vazquez Noguera, "Top-hat transform for enhancement of aerial thermal images," in *Proc. 30th SIBGRAPI Conf. Graph., Patterns Images (SIBGRAPI)*, Oct. 2017, pp. 277–284.
[38] N. Al-Najdawi, M. Biltawi, and S. Tedmori, "Mammogram image visual enhancement, mass segmentation and classification," *Appl. Soft Comput.*, vol. 35, pp. 175–185, Oct. 2015.
[39] T. Hopp, M. Dietzel, P. Baltzer, P. Kreisel, W. A. Kaiser, H. Gemmeke, and N. Ruiter, "Automatic multimodal 2D/3D breast image registration using biomechanical FEM models and intensity-based optimization," *Med. Image Anal.*, vol. 17, 2, pp. 209–218, 2013.
[40] D. Chandler, "Seven challenges in image quality assessment: Past, present, and future research," *Int. Scholarly Res. Notices*, vol. 2013, pp. 1–53, Mar. 2013.
[41] J.-F. Pambrun and R. Noumeir, "Limitations of the SSIM quality metric in the context of diagnostic imaging," in *Proc. IEEE Int. Conf. Image Process. (ICIP)*, Sep. 2015, pp. 2960–2963.
[42] M. Outtas, L. Zhang, O. Deforges, W. Hammidouche, A. Serir, and C. Cavaro-Menard, "A study on the usability of opinion-unaware no-reference natural image quality metrics in the context of medical images," in *Proc. Int. Symp. Signal, Image, Video Commun. (ISIVC)*, 2016, pp. 308–313.
[43] C. Cavaro-Menard, L. Zhang, and P. Le Callet, "Diagnostic quality assessment of medical images: Challenges and trends," in *Proc. 2nd Eur. Workshop Vis. Inf. Process. (EUVIP)*, Jul. 2010, pp. 277–284.
[44] M. A. Qureshi, A. Beghdadi, and M. Deriche, "Towards the design of a consistent image contrast enhancement evaluation measure," *Signal Process., Image Commun.*, vol. 58, pp. 212–227, Oct. 2017.
[45] M. A. Qureshi, M. Deriche, A. Beghdadi, and M. Mohandes, "An information based framework for performance evaluation of image enhancement methods," in *Proc. Int. Conf. Image Process. Theory, Tools Appl. (IPTA)*, Nov. 2015, pp. 519–523.
[46] Z. A. Khan, A. Beghdadi, F. A. Cheikh, M. Kaaniche, and M. Ali Qureshi, "A multi-criteria contrast enhancement evaluation measure using wavelet decomposition," in *Proc. IEEE 22nd Int. Workshop Multimedia Signal Process. (MMSP)*, Sep. 2020, pp. 1–6.
[47] Y. Zhang, B. Jiang, J. Wu, D. Ji, Y. Liu, Y. Chen, E. X. Wu, and X. Tang, "Deep learning initialized and gradient enhanced level-set based segmentation for liver tumor from CT images," *IEEE Access*, vol. 8, pp. 76056–76068, 2020.
[48] G. Lin, W. Wang, C. Kang, and C. Wang, "Multispectral MR images segmentation based on fuzzy knowledge and modified seeded region growing," *Magn. Reson. Imag.*, vol. 30, 2, pp. 230–246, 2012.
[49] D. Dreizin, U. K. Bodanapally, N. Neerchal, N. Tirada, M. Patlas, and E. Herskovits, "Volumetric analysis of pelvic hematomas after blunt trauma using semi-automated seeded region growing segmentation: A method validation study," *Abdominal Radiol.*, vol. 41, no. 11, pp. 2203–2208, Nov. 2016.
[50] J. Lian, Y. Ma, Y. Ma, B. Shi, J. Liu, Z. Yang, and Y. Guo, "Automatic gallbladder and gallstone regions segmentation in ultrasound image," *Int. J. Comput. Assist. Radiol. Surg.*, vol. 12, no. 4, pp. 553–568, Apr. 2017.
[51] G. N. Harikrishna Rai and T. R. Gopalakrishnan Nair, "Gradient based seeded region grow method for CT angiographic image segmentation," 2010, *arXiv:1001.3735*. [Online]. Available: http://arxiv.org/abs/1001.3735

RABIA NASEEM received the master's degree in software engineering from the University of Engineering and Technology, Taxila, Pakistan. She is currently pursuing the Ph.D. degree with the Department of Computer Science, Norwegian University of Science and Technology, Norway. She is also working as a Marie Curie Fellow under the European Union-Funded Project High-Performance Soft Tissue Navigation and her research interests include medical image processing, particularly medical image enhancement and deep learning.

ZOHAIB AMJAD KHAN (Student Member, IEEE) received the dual master's degree in information and communication technologies from the Politecnico di Torino, Italy, and Karlsruhe Institute of Technology, Germany, in 2010. He has been a Ph.D. Researcher working at the Institut Galilée, Université Sorbonne Paris Nord, France, since 2017. His research interests include medical imaging, image and video processing and quality assessment, applied deep learning, and virtual reality simulations.

NITIN SATPUTE received the M.E. degree in embedded systems from BITS Pilani, India, and the Ph.D. degree (Hons.) in computer science from the University of Cordoba, Spain. Before joining AU, he was a Marie Curie Researcher under the HiPerNav Project funded by the European Union (EU) at the University of Cordoba. He is currently a Postdoctoral Researcher in machine learning and computational intelligence with Aarhus University (AU), Denmark. He is also involved in the fast efficient distributed training for deep neural networks (DNN). His research interests include AI, parallel computing, medical image analysis, and automated crowd management systems.

AZEDDINE BEGHDADI (Senior Member, IEEE) received the master's degree in optics and signal processing from Paris-Saclay University, in June 1983, and the Ph.D. degree in physics specialization in optics and signal processing from Sorbonne University, in June 1986. He has been a Full Professor with University Sorbonne Paris Nord (USPN), since 2000. He is currently the Founding Member of the Laboratory of Information Processing and Transmission (L2TI laboratory), and was its Director, from 2010 to 2016. He worked at different places during his Ph.D. thesis, including the Laboratoire d'Optique des Solides (University Pierre et Marie Curie—Sorbonne University) and Groupe d'Analyse d'Images Biomédicales (CNAM Paris). From 1987 to 1989, he held the position of a Lecturer at USPN. During the period 1987 to 1998, he was with the LPMTM-CNRS Laboratory working on scanning electron microscope materials image analysis. He has published over more than 300 international refereed scientific papers. His research interests include image/video quality enhancement and assessment, bio-inspired models for image analysis and processing, and machine learning. He is an Elected Member of IEEE-MMSP TC and EURASIP VIP-TAC. He also served as a session organizer and a member for the organizing and technical committees for many IEEE conferences. He served as the conference chair and the technical chair for many international conferences. He is a EURASIP Member and IEEE-MMTC Member. He is the Founder and the Steering Committee Chair of the European Workshop on Visual Information Processing (EUVIP). He is an Associate Editor of *Signal processing: Image Communication* journal (Elsevier), *European Journal on Image and Video Processing* (Springer, Verlag), and *Mathematical Problems in Engineering* journal (Hindawi).

FAOUZI ALAYA CHEIKH (Senior Member, IEEE) received the Ph.D. degree in information technology from Tampere University of Technology, Tampere, Finland, in April 2004. He had worked as a Researcher with the Signal Processing Algorithm Group, Tampere University of Technology, in 1994. Since 2006, he has been affiliated with the Department of Computer Science and Media Technology, Gjøvik University College, Norway, as an Associate Professor. Since January 2016, he has also been with the Norwegian University of Science and Technology (NTNU). He teaches courses on image and video processing and analysis and media security. He is currently the co-supervisor of five Ph.D. students. He has been involved in several European and national projects, such as ESPRIT, NOBLESS, COST 211Quat, HyPerCept, IQ-Med, and H2020 ITN HiPerNav. His research interests include e-Learning, 3-D imaging, image and video processing and analysis, video-based navigation, biometrics, pattern recognition, embedded systems, and content-based image retrieval. In these areas, he has published over 100 peer-reviewed journal articles and conference papers, and supervised four postdoctoral researchers, five Ph.D., and a number of M.Sc. thesis projects. He is a member of NOBIM and Forskerforbundet [The Norwegian Association of Researchers (NAR)]. He is on the Editorial Board of the *IET Image Processing Journal* and the *Journal of Advanced Robotics & Automation*, and the technical committees of several international conferences. He is an expert reviewer to a number of scientific journals and conferences related to the field of his research.

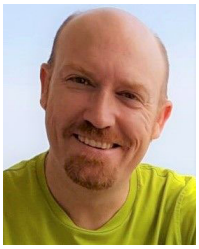

JOAQUÍN OLIVARES received the B.S. and M.S. degrees in computer sciences and the M.S. degree in electronics engineering from the Universidad de Granada, Spain, in 1997, 1999, and 2003, respectively, and the Ph.D. degree from the Universidad de Córdoba, Spain, in 2008. He has been an Associate Professor with the Department of Electronic and Computer Engineering, Universidad de Córdoba, since 2001. He is currently the Founder and the Head of the Advanced Informatics Research Group. His research interests include the field of the Internet of Things, embedded systems, computer vision, and high performance computing.